

An Image Analysis Framework for the Early Assessment of Hypertensive Retinopathy Signs

G. Manikis¹, V. Sakkalis¹, X. Zabulis¹,
P. Karamaounas¹, A. Triantafyllou², S. Douma²,
Ch. Zampoulis² and K. Marias¹

(¹) Foundation for Research & Technology (FORTH)

(²) Hypertension Unit, 2nd Propaedeutic Dept. of Internal Medicine,
Hippokration Hospital, Aristotle University of Thessaloniki, Hellas



Introduction

- This study presents a **framework for the detection and measurement of retinal vessels in funduscopy images.**
 - The development of advanced fundus cameras along with image processing techniques offer an **accurate, objective, and repeatable** representation of retinal blood vessels.
 - Retinal vessels can be easily visualized with non-invasive techniques providing valuable information in the **diagnosis, classification and surveillance of retinopathy** signs.
- In this study, a method was implemented to segment retinal vessels, enabling the actual measurement of the vessel diameter, along with a
 - Graphical User Interface (GUI) to support automatic and interactive measurement of vessel diameters at any selected point or region of interest. Editing the vessel representation in order to recover from possible segmentation misclassifications.
- The proposed methodology may support vascular risk stratification in persons with hypertension.

Experimental Data

- Our main aim was to provide a tool which assists the clinician to handle High Resolution (HR) raw retinal images. Therefore, 10 images of size 2912X2912 were acquired.
- In order to verify the applicability of the proposed scheme in lower resolutions we evaluated our methodology on two publicly available datasets;
 - DRIVE ^[1]: 40 retinal images along with manual segmentations of the vessels with size of 768X584
 - STARE ^[2]: 20 digitized slides to 700X605
- Many of the post-processing steps were applied only to HR images

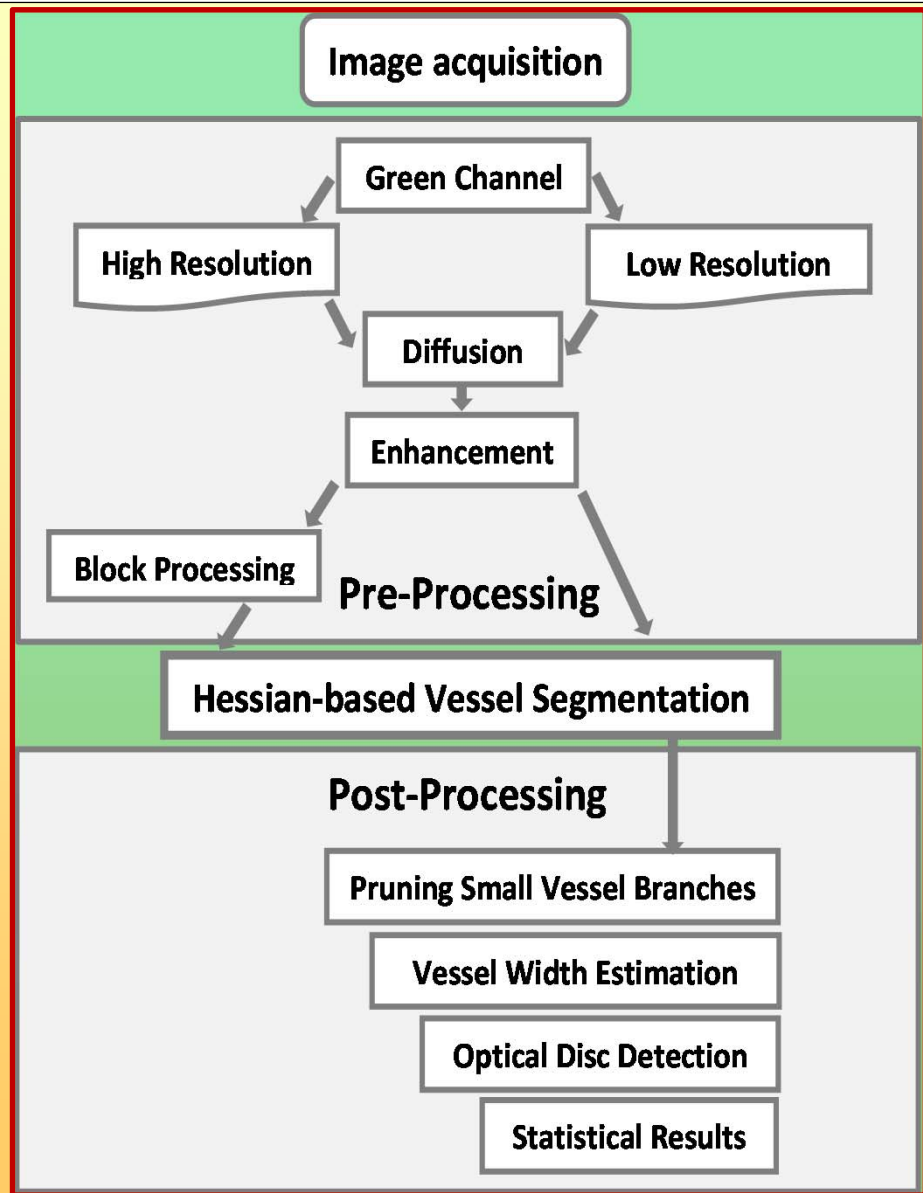


Flowchart of the framework

The applied techniques are illustrated as a pipeline of processes consisting of two separate modules.

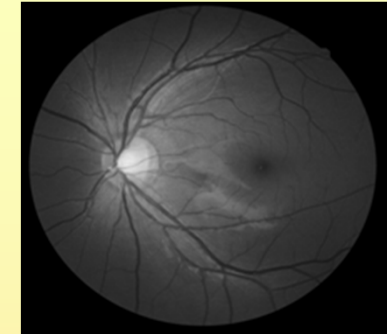
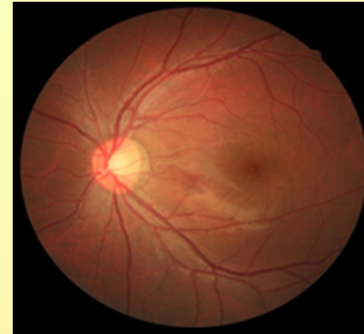
- The first includes the detection and measurement of vessels in retinal images.
- The second provides the ability to validate, edit and represent vessel information in multiple ways, by interactively selecting segments of interest and extracting their statistical information within spatial regions.

A GUI encapsulates both modules and increases the automation and usability of the measurement process.

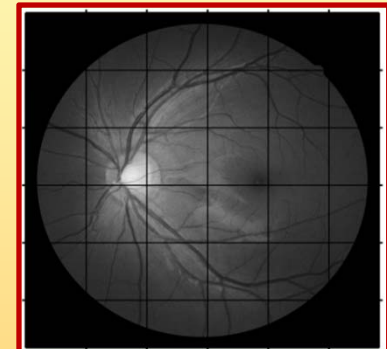
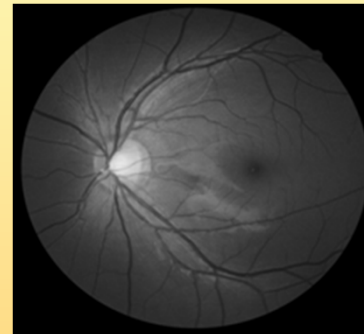


Pre-Processing 1/2

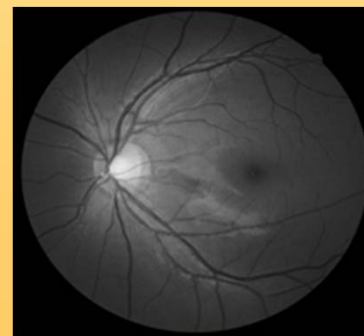
The **green channel** of the retinal image was extracted for use as it provides the greatest contrast for blood vessels. The acquired retinal images were transformed from **colored to monochromatic**.



HR Image processing was implemented through **distinct blocking**. Processing HR images was a computationally daunting task where most algorithms fail to achieve because of **memory constraints**.

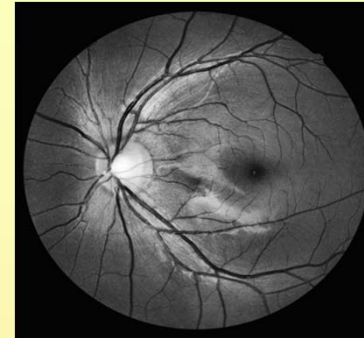


An edge-preserving **anisotropic diffusion filter** [3] was applied to smooth the images within homogeneous regions. Then, the smoothed image was enhanced using a contrast limited adaptive **histogram equalization** [4].

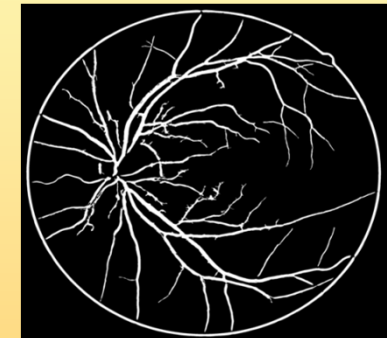


Pre-Processing 2/2

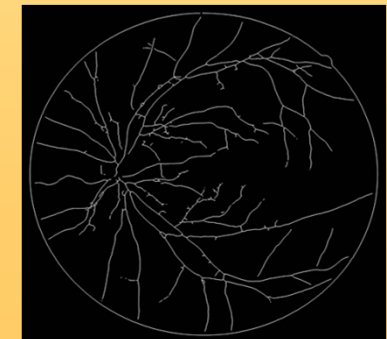
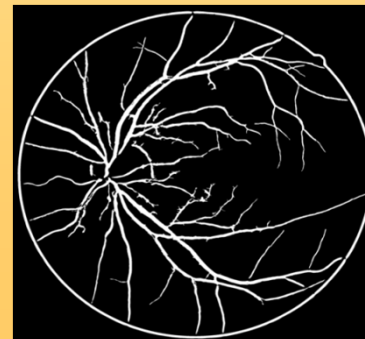
We then incorporated a **multiple scale filtering technique** for vessel enhancement, based on the eigenvalue analysis of the **Hessian matrix** [5] for vessel enhancement.



An **iterative thresholding** method for segmenting the blood vessel structure was then applied for the **binarization** of the image. We focused on segmentation techniques that balance between accuracy and complexity and **Otsu's thresholding** [6] acted fairly well under those requirements.



Finally, the **skeletonization** of the segmented image was required for the characterization of the **morphological structure** of the blood vessel's network.



Evaluation of the Technique in LR Images

- To facilitate the comparison with other well-known retinal vessel segmentation approaches the performance of the proposed method was evaluated on the **DRIVE** and **STARE** datasets.
- LR images contribute only to the pre-processing approach in order to assess the quality of the segmented and skeletonized images before entering the post-processing phase.

Performance of vessel segmentation - DRIVE				
	Method	Sensitivity	Specificity	Accuracy
	Human Observer	0.7761	0.9725	0.9473
Supervised Methods	Soares [7]	0.7230	0.9762	0.9446
	Staal [1]	0.7193	0.9773	0.9441
	Niemeijer [8]	0.6793	0.9801	0.9416
Unsupervised Methods	Mendonca [9]	0.7344	0.9764	0.9452
	Proposed	0.7414	0.9669	0.9371
	Vlachos [10]	0.7468	0.9551	0.9285
	Jiang [11]	0.6478	0.9625	0.9222
	Perez [12]	0.7086	0.9496	0.9181
	Chaudhuri [13]	0.2716	0.9794	0.8894
Performance of vessel segmentation - STARE				
	Method	Sensitivity	Specificity	Accuracy
	Human Observer	0.8949	0.9390	0.9354
Supervised Methods	Staal [1]	0.6970	0.9810	0.9516
	Soares [7]	0.7103	0.9737	0.9480
Unsupervised Methods	Mendonca [9]	0.6996	0.9730	0.9440
	Perez [12]	0.7506	0.9569	0.9410
	Proposed	0.7189	0.9656	0.9318

Post-Processing 1/3

Size-based filtering:

The first stage of the post-processing procedure is to delete very small isolated skeleton segments as they typically correspond to noise artifacts.

Pruning small vessel branches:

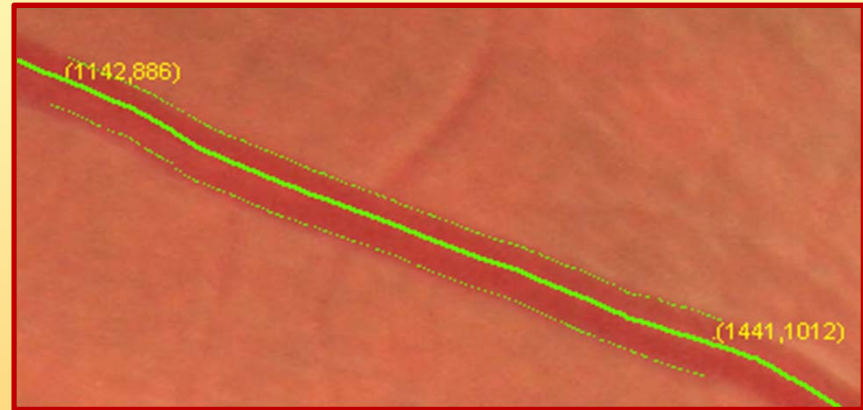
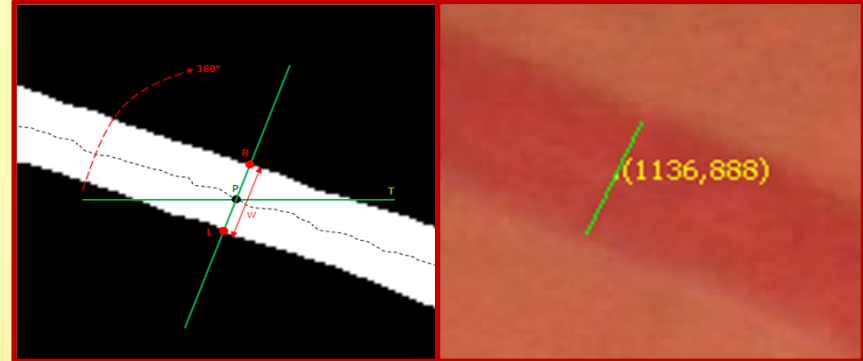
The segmentation results obtained from HR images tend to exhibit a rich structure at vessel boundaries. In HR images such structures give rise to spurious skeleton branches. The effect of filtering the branches provided a more accurate representation of vessels, particularly because vessel branching points convey important information in measurements, according to the particular medical protocol.



Post-Processing 2/3

Vessel width estimation:

- First, a local algorithm is employed to estimate the vessel width at a skeleton point p , using both the segmented and the skeleton images.
- Then, the user provides two input points for measuring the mean vessel width along a segment of a vessel.
- The system finally retrieves the skeleton points of the segment in between the two points along with their estimated widths and averages them.



Optical disc detection:

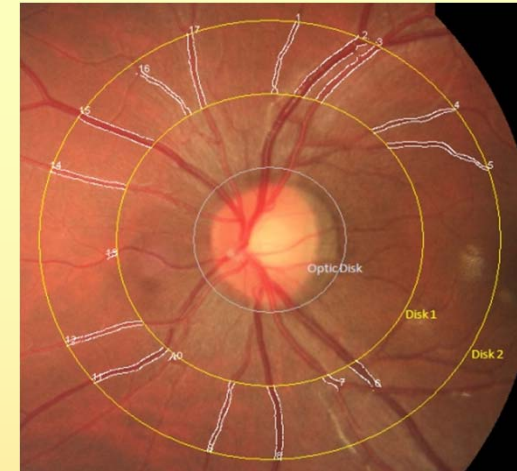
- Optic disk is automatically detected in the acquired image and estimate of its size is provided. In this way, the application of medical protocols that are based on measurements around this disk can be automated.



Post-Processing 3/3

Measuring multiple vessel segments :

The measurement of average width of multiple non-branching vessels, at a range of distances from the center of the optical disk is performed. Each vessel segment initiates from the smaller to the larger circle. Depending on user selection, a number of statistics can be then estimated.



Statistical Analysis in HR Images:

The ratio of the quantities, CRAE and CRVE [14], which are determined by measurement on the arteries and veins detected in the region of interest respectively, were estimated. Such measures require the characterization of vessels, as to if they are veins or arteries and their mean widths. Hence, a GUI component is provided to facilitate this characterization by the medical professional.

Points	Width	fix	Kind
1. Points: 265	Width: 311.673	fix 311.673	Kind: <input type="radio"/> Arteriole <input type="radio"/> Venule <input type="radio"/> Capillary
2. Points: 239	Width: 862.306	fix 862.306	Kind: <input type="radio"/> Arteriole <input type="radio"/> Venule <input type="radio"/> Capillary
3. Points: 229	Width: 565.391	fix 565.391	Kind: <input type="radio"/> Arteriole <input type="radio"/> Venule <input type="radio"/> Capillary
4. Points: 286	Width: 374.044	fix 374.044	Kind: <input type="radio"/> Arteriole <input type="radio"/> Venule <input type="radio"/> Capillary
5. Points: 346	Width: 377.634	fix 377.634	Kind: <input type="radio"/> Arteriole <input type="radio"/> Venule <input type="radio"/> Capillary
6. Points: 26	Width: 198.822	fix 198.822	Kind: <input type="radio"/> Arteriole <input type="radio"/> Venule <input type="radio"/> Capillary
7. Points: 117	Width: 694.587	fix 694.587	Kind: <input type="radio"/> Arteriole <input type="radio"/> Venule <input type="radio"/> Capillary
8. Points: 74	Width: 572.163	fix 572.163	Kind: <input type="radio"/> Arteriole <input type="radio"/> Venule <input type="radio"/> Capillary
9. Points: 271	Width: 565.350	fix 565.35	Kind: <input type="radio"/> Arteriole <input type="radio"/> Venule <input type="radio"/> Capillary
10. Points: 259	Width: 351.497	fix 351.497	Kind: <input type="radio"/> Arteriole <input type="radio"/> Venule <input type="radio"/> Capillary
11. Points: 23	Width: 367.607	fix 367.607	Kind: <input type="radio"/> Arteriole <input type="radio"/> Venule <input type="radio"/> Capillary
12. Points: 262	Width: 477.055	fix 400	Kind: <input type="radio"/> Arteriole <input type="radio"/> Venule <input type="radio"/> Capillary
13. Points: 271	Width: 382.833	fix 382.833	Kind: <input type="radio"/> Arteriole <input type="radio"/> Venule <input type="radio"/> Capillary
14. Points: 271	Width: 357.199	fix 350	Kind: <input type="radio"/> Arteriole <input type="radio"/> Venule <input type="radio"/> Capillary
15. Points: 264	Width: 460.821	fix 460.821	Kind: <input type="radio"/> Arteriole <input type="radio"/> Venule <input type="radio"/> Capillary
16. Points: 259	Width: 635.966	fix 635.966	Kind: <input type="radio"/> Arteriole <input type="radio"/> Venule <input type="radio"/> Capillary
17. Points: 199	Width: 317.078	fix 317.078	Kind: <input type="radio"/> Arteriole <input type="radio"/> Venule <input type="radio"/> Capillary
18. Points: 272	Width: 490.698	fix 490.698	Kind: <input type="radio"/> Arteriole <input type="radio"/> Venule <input type="radio"/> Capillary

User Interface Overview

Semi-automatic pre-processing:

The purpose of implementing this functionality is threefold;

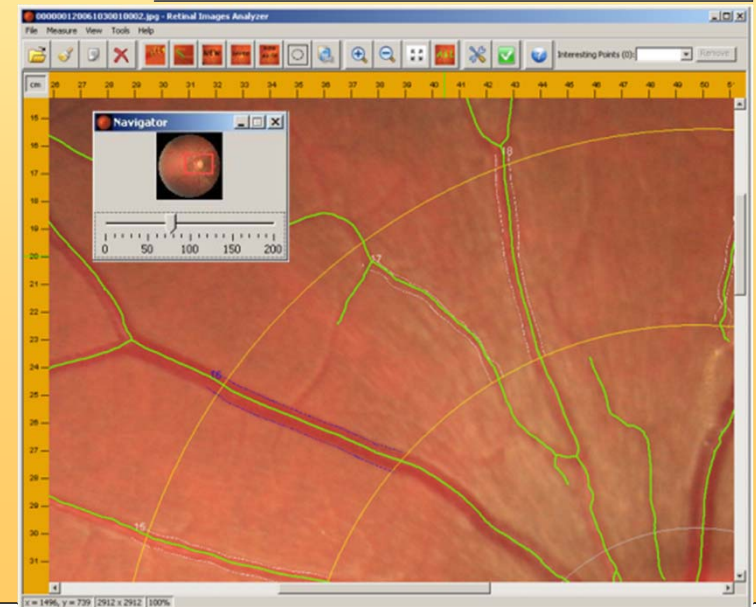
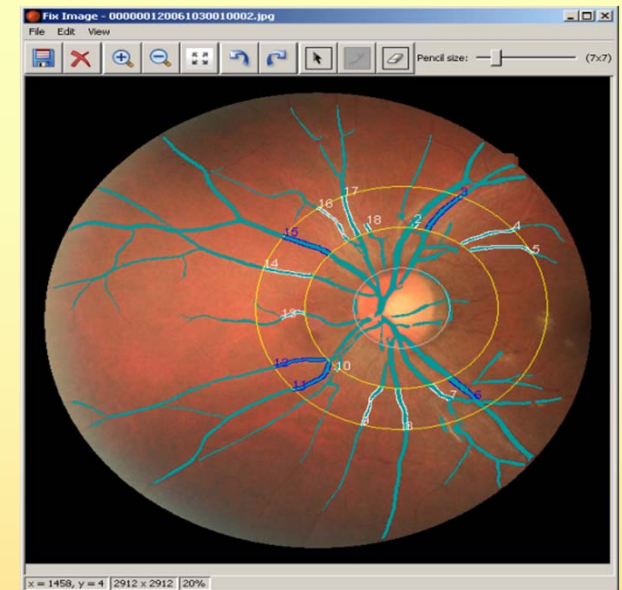
- user can manually corrects remaining errors in the segmentation image
- performs targeted measurements (i.e. focuses on a particular vessel and ignore its branches)
- acquire ground truth results by superimposing a basis segmented image to the original image.

Other utilities:

Saving of data file with measurements, reviewing and editing of old measurement files.

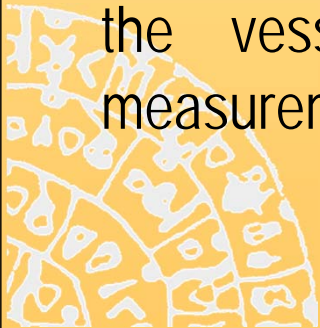
Image view allowing measurement and skeleton points calculation using magnification options (visible image segment in thumbnail view).

Rulers display allowing calibrated grid measurements.



Conclusions

- The presented application employs an **image segmentation algorithm**, along with **pre-processing** and **skeletonization** techniques in order to extract a representation of vessels.
- Additionally, techniques that analyze this representation and **measure vessel width** are introduced and adapted appropriately, in order to provide measurements according to particular measurement protocols.
- The above functionalities are **integrated through a GUI**, which assists the medical professional to perform measurements in an ergonomic fashion and apply targeted measurements.
- This interface provides also functionalities that allow the clinician to edit the vessel segmentation result and update the corresponding measurements, in order to recover from segmentation errors.



Future Work

- Future work will be pursued along two research avenues.
 - The first regards the **improvement of the segmentation algorithm.**
 - The second regards the **registration of fundoscopy images of the same patient, acquired across large time intervals.**
- The goal is to **provide medical professionals with the capability of automatically comparing vessel measurements, thus offering a valuable tool in the monitoring, diagnosis, and estimation of the condition of the cardiovascular system.**



References

1. Staal, J.; Abramoff, M.D.; Niemeijer, M.; Viergever, M.A.; van Ginneken, B.; , "Ridge-based vessel segmentation in color images of the retina," *Medical Imaging, IEEE Transactions on* , vol.23, no.4, pp.501-509, April 2004.
2. A. Hoover, V. Kouznetsova, and M. Goldbaum, "Locating blood vessels in retinal images by piecewise threshold probing of a matched filter response," *IEEE Trans. Med. Imag.*, vol. 19, no. 3, pp. 203–211, Mar. 2000.
3. P. Perona, J. Malik, "Scale-space and edge detection using anisotropic diffusion," *IEEE Trans. PAMI*, V. 12, no. 7, pp. 629-639, July 1990.
4. K. Zuiderveld. Contrast limited adaptive histogram equalization. *Graphics gems IV*, pages 474-485, 1994.
5. A.F. Frangi, W.J. Niessen, K.L. Vincken, M.A. Viergever (1998). Multiscale vessel enhancement filtering. In *Medical Image Computing and Computer-Assisted Intervention - MICCAI'98*, W.M. Wells, A. Colchester and S.L. Delp (Eds.), *Lecture Notes in Computer Science*, vol. 1496 - Springer Verlag, Berlin, Germany, pp. 130-137.
6. Otsu, N., "A Threshold Selection Method from Gray-Level Histograms," *IEEE Transactions on Systems, Man, and Cybernetics*, Vol. 9, No. 1, 1979, pp. 62-66.
7. João V. B. Soares, Jorge J. G. Leandro, Roberto M. Cesar Jr., Herbert F. Jelinek, and Michael J. Cree, "Retinal Vessel Segmentation Using the 2-D Gabor Wavelet and Supervised Classification," *IEEE Transactions on medical Imaging*, vol. 25, no. 9, September 2006.
8. Niemeijer M., Staal J., van Ginneken B, Loog M, and Abramoff M. D., "Comparative study of retinal vessel segmentation methods on a new publicly available database," in *Proc. SPIE Med. Imag.*, M. Fitzpatrick and M. Sonka, Eds., 2004, vol. 5370, pp. 648–656.
9. A. Mendonca and A. Campilho. Segmentation of retinal blood vessels by combining the detection of centerlines and morphological reconstruction. *IEEE Transactions on Medical Imaging*, 25(9):1200-1213, September 2006.
10. M. Vlachos, E. Dermatas, Multi-scale retinal vessel segmentation using line tracking, *Computerized Medical Imaging and Graphics*, Volume 34, Issue 3, April 2010, Pages 213-227.
11. Xiaoyi Jiang; Mojon, D.; , "Adaptive local thresholding by verification-based multithreshold probing with application to vessel detection in retinal images," *Pattern Analysis and Machine Intelligence, IEEE Transactions on* , vol.25, no.1, pp.131-137, Jan. 2003.
12. M.E. Martínez-Pérez, A.D. Hughes, A.V. Stanton, S.A. Thom, A.A. Bharath, and K.H. Parker, "Retinal Blood Vessel Segmentation by Means of Scale-Space Analysis and Region Growing", in *Proc. MICCAI*, 1999, pp.90-97.
13. S. Chaudhuri, S. Chatterjee, N. Katz, M. Nelson, and M. Goldbaum, "Detection of blood vessels in retinal images using two-dimensional matched filters," *IEEE Trans. Med. Imag.*, pp. 263–269, 1989.
14. Hubbard LD, Brothers RJ, King WN, Clegg LX, Klein R, Cooper LS, et al. Methods for evaluation of retinal microvascular abnormalities associated with hypertension/sclerosis in the Atherosclerosis Risk in Communities Study. *Ophthalmology*;106(12):2269-80, Dec 1999.

Acknowledgments

- The authors would like to thank the Hypertension Unit of the 2nd Propaedeutic Dept. of Internal Medicine, Hippokration Hospital in Thessaloniki for providing the High Resolution dataset.
- This work was supported in part by the European Commission under the TUMOR (FP7-ICT-2009.5.4-247754) project.

Thank you

Vangelis Sakkalis
sakkalis@ics.forth.gr